



PERGAMON

Available online at www.sciencedirect.com

SCIENCE @ DIRECT®

Polyhedron 22 (2003) 2301–2305



POLYHEDRON

www.elsevier.com/locate/poly

Spin-density distribution of the high T_c p -O₂N·C₆F₄·CNSSN free radical studied by polarised neutron diffraction

Javier Luzón^a, Javier Campo^{a,b,*}, Fernando Palacio^b, Garry J. McIntyre^a,
Andrés E. Goeta^c, Christopher M. Pask^d, Jeremy M. Rawson^d

^a Institut Laue Langevin, 6 rue Jules Horowitz, 38042 Grenoble, France

^b Instituto de Ciencia de Materiales de Aragón, CSIC-Universidad de Zaragoza, Pedro Cerbuna 12, 50009 Zaragoza, Spain

^c Chemistry Department, Durham University, Durham, UK

^d Department of Chemistry, University of Cambridge, Cambridge CB2 1EW, UK

Received 7 October 2002; accepted 24 January 2003

Abstract

Knowledge of the spin-density distribution in the dithiadiazolyl radical ring (DTDA) constitutes a major step towards the understanding of the magnetic and electronic properties of the rich magnetism of DTDA derivatives. The p -O₂N·C₆F₄·CNSSN[•] radical was chosen as the most favourable CNSSN[•] derivative to study the spin distribution in this kind of free radical by polarised neutron diffraction. Spin-density maps obtained for the p -O₂N·C₆F₄·CNSSN[•] radical show that almost all the spin density is localised on the sulphur and nitrogen atoms of the CNSSN[•] ring. A small negative spin density on the carbon atom of the CNSSN[•] ring and a negligible spin density over the rest of the radical are observed, in good agreement with ab initio calculations.

© 2003 Elsevier Science Ltd. All rights reserved.

Keywords: Spin densities; Molecular magnet; Magnetic interactions

1. Introduction

In recent years, there has been considerable interest in the study of the magnetic behaviour of free radicals [1]. Part of such interest has been focused on the development and study of organic materials that exhibit spontaneous magnetisation on decreasing temperature in order to develop organic ferromagnets free of metallic elements. Such materials can exhibit peculiar and probably unprecedented properties not shown by the traditional inorganic magnetic materials based on metallic or ionic lattices: low density, transparency, photo-responsiveness, electrical insulation, bio-compatibility, low-temperature fabrication, easy processability, etc. Furthermore, a most interesting characteristic of these materials is the possibility of performing slight chemical

modifications to change their physical properties. This opens a wide range of practical possibilities to address fundamental questions such as which are the dominant mechanisms for the propagation of magnetic interaction and even for the molecular packing itself. The conditions required not only to stabilise an organic free radical in the solid state but also to control its molecular packing in order to produce magnetic ordering are difficult to fulfil. Moreover, the tendency of free radicals to interact antiferromagnetically favours antiferromagnetic rather than ferromagnetic ordering.

Thus far very few organic ferromagnets have been reported. The first neutral free radical ferromagnet was reported in 1991 as the β -phase of p -nitrophenyl nitronyl nitroxide which orders at 0.6 K [2,3]. Simultaneously, ferromagnetism was also identified at 16 K in the ionic complex radical TDAE–C₆₀ [4]. A second neutral free radical ferromagnet, the nitroxide biradical DOTMDAA, was reported in 1993 to exhibit a Curie temperature of 1.48 K [5].

The dithiadiazolyl radicals X·C₆F₄·CNSSN[•] (X = Br, O₂N, CN, etc.) are free radicals with an unpaired

* Corresponding author. Present address: Instituto de Ciencia de Materiales de Aragón, CSIC-Universidad de Zaragoza, Pedro Cerbuna 12, 50009 Zaragoza, Spain. Tel.: +34-976-76-27-42; fax: +34-976-76-12-29.

E-mail address: jcampo@unizar.es (J. Campo).

electron delocalised in the CNSSN• ring. The CN·C₆F₄·CNSSN• radical has been reported as a weak ferromagnet with an ordering temperature of 36 K [6]. This temperature is the highest ordering temperature observed in a purely organic magnet to date.

Several substitutions of the CN group in the NC·C₆F₄·CNSSN• radical have been made. The result is a major change in the molecular packing and, consequently, a substantial modification of the magnetic properties. Thus, by changing the CN group by Br a paramagnetic system possessing very weak antiferromagnetic interactions was obtained. However, if the CN group is substituted by O₂N to give the O₂N·C₆F₄·CNSSN• radical ferromagnetic ordering is observed below $T_c = 1.3$ K [7].

On the other hand, ab initio calculations have shown that the unpaired electron density in CN·C₆F₄·CNSSN• radical is on a molecular orbital localised on the CNSSN ring and that the spin-density distribution does not depend on the particular X group.

We report herein a single-crystal polarised neutron study of the spin density in the CNSSN• ring, together with ab initio calculations, as a step towards the understanding of the magnetic and electronic properties of these compounds. The compound chosen for the experiment was the O₂N·C₆F₄·CNSSN• radical, which is paramagnetic above 1.3 K.

2. Experimental

2.1. Nuclear structure at low temperature

The radical, *p*-O₂N·C₆F₄·CNSSN was synthesised from *p*-O₂N·C₆F₄·CN utilising standard synthetic procedures and crystallised by sublimation in vacuum (100–70 °C, 0.1 mmHg) [7]. Large crystals up to 1 × 1 × 1 mm³ could be grown by annealing a sample in vacuo at ca. 120 °C for 4 h. The structure of O₂N·C₆F₄·CNSSN• was known from X-ray diffraction experiments at room temperature [7]. In order to obtain the crystal structure in detail at low temperature and determine the degree of extinction and multiple scattering in the particular crystal used, an unpolarised neutron experiment was performed at 20 K on the 4-circle diffractometer D9 at the Institut Laue Langevin (ILL) in Grenoble, France. A wavelength of 0.8401 Å was used to collect 1463 independent reflections from a crystal of 1 × 1 × 1 mm³ volume. Appropriated absorption, extinction, Lorentz geometrical and multiple scattering corrections were applied to the measured intensities to determine the F_N^2 values, where F_N are the nuclear structure factors. Programs from the CCSL suite [8] were used to analyse the data and refine the structural model.

2.2. Polarised neutron diffraction experiment

The polarised neutron diffraction technique consists of determining the flipping ratios $R(hkl)$, between the diffracted intensities, I^{up} and I^{down} , at the Bragg peak measured for a incident neutron beam polarised up or down, respectively. That flipping ratio for each hkl reflection is related to the nuclear $F_N(hkl)$ and magnetic $F_M(hkl)$ structure factors. Assuming that all magnetic moments in the sample are oriented in the same direction, parallel to the beam polarisation, the expression for $R(hkl)$ can be simplified as:

$$R = \frac{I^{\text{up}}}{I^{\text{down}}} = \frac{F_N'^2 + F_N''^2 + 2p \sin^2 \alpha (F_N' F_M' + F_N'' F_M'') + \sin^2 \alpha (F_M'^2 + F_M''^2) + A}{F_N'^2 + F_N''^2 - 2ep \sin^2 \alpha (F_N' F_M' + F_N'' F_M'') + \sin^2 \alpha (F_M'^2 + F_M''^2) + B} \quad (1)$$

where F_N' , F_N'' , F_M' , F_M'' are the real and imaginary parts of the nuclear and magnetic structure factors, respectively, α the angle between the reflection hkl and the magnetic moments in the sample, p the up-polarisation of the beam and ep the down-polarisation. A and B terms take into account different corrections for $\lambda/2$ contributions, multiple scattering and the Schwinger effect. Eq. (1) has two unknown quantities F_M' and F_M'' that cannot be extracted directly from the flipping ratio. In the particular case, where the nuclear structure is centric, then F_M'' is null and therefore from Eq. (1) the magnetic structure factor can be determined. If the nuclear structure is acentric then, as will be explained later, the data analysis process directly the flipping ratios.

The polarised neutron diffraction experiments were performed on the D3 lifting-counter-diffractometer at the ILL. A Heusler crystal was used to monochromate the incoming neutron beam at a wavelength of 0.843 Å with a polarisation of 0.93. A cryoflipper with 100% efficiency changed the polarisation between up and down relative to the vertical magnetic field applied to the sample.

For this experiment, the same crystal mounted on D9 was used. Due to the crystal size and to the small magnetic density about 30 min of accumulation time per peak were necessary in order to obtain good statistics. The magnetic flipping ratios of only 128 independent reflections from 294 total reflections, covering a $\sin \theta/\lambda$ range of 0.72 Å⁻¹, could be measured in the time available for the experiment. The experimental temperature was set at 1.5 K with an applied field of 9 T.

3. Results and discussion

3.1. Structural study

Only reflections with $F_N > 3\sigma$ were considered for the nuclear refinement. Position and anisotropic thermal parameters for all atoms were refined. Structural details corresponding to the low-temperature structure will be provided in a more complete paper elsewhere and only relevant facts are mentioned here.

The $p\text{-O}_2\text{N}\cdot\text{C}_6\text{F}_4\cdot\text{CNSSN}^\bullet$ radical crystallises in the tetragonal space group $P4_12_12$ with cell parameters $a = 8.1125 \text{ \AA}$, $c = 14.764 \text{ \AA}$ at low temperature and four molecules for unit cell arranged in planes perpendicular to the c -axis and rotated 90° with respect to each other. Nuclear symmetry is preserved all the way from RT to 1.5 K. The structure consists of infinite chains of monomeric radicals packed in a head-to-tail arrangement that are not related by an inversion centre as it is shown in Fig. 1. The absence of an inversion centre between interacting molecules allows the presence of a Dzyaloshinskii–Moriya (DM) term in the interaction Hamiltonian. Although such term is necessarily very weak, it can be sufficient to move slightly the magnetic moments in the radical molecules away from parallel arrangement. The DM term is responsible for the weak ferromagnetism in the $p\text{-CN}\cdot\text{C}_6\text{F}_4\cdot\text{CNSSN}^\bullet$ radical where a canting angle from collinear antiferromagnetic arrangement of less than 0.1° was determined [6]. Given that the $p\text{-O}_2\text{N}\cdot\text{C}_6\text{F}_4\cdot\text{CNSSN}^\bullet$ radical is ferromagnetic, a canting angle of about 0.1° would be undetectable.

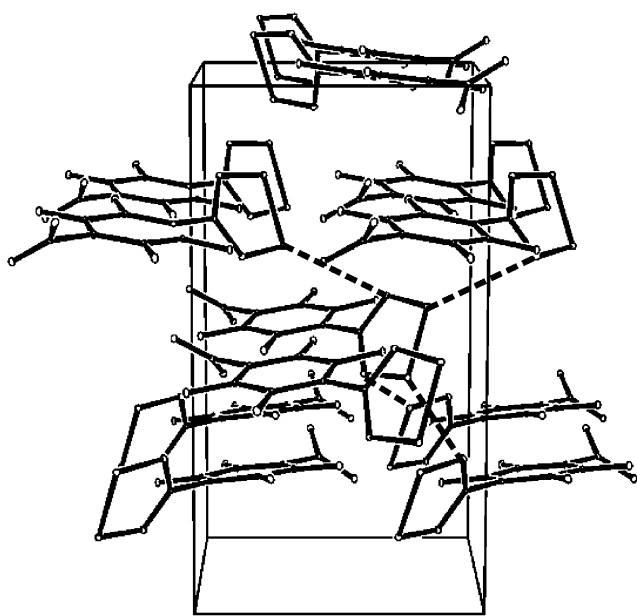


Fig. 1. View of the crystal structure of $\text{O}_2\text{N}\cdot\text{C}_6\text{F}_4\cdot\text{CNSSN}^\bullet$ radical. The dotted lines indicate the four proposed exchange pathways.

3.2. Ab initio calculations

In order to understand the measured spin-density, a theoretical study was done. Various methods are available; here we report results of DFT calculations using the BYLP correlation exchange functional [9]. That calculations allow us to calculate the magnetic ground state of the $p\text{-O}_2\text{N}\cdot\text{C}_6\text{F}_4\cdot\text{CNSSN}^\bullet$ radical. The DMOL3 program [10] using periodic conditions and a basis set of double numeric functions with polarisation was employed in the calculations. The Mulliken population obtained from these calculations are shown in Table 1 together with experimental values for comparison.

3.3. Spin-density reconstruction

In Figs. 2 and 3 are shown the projections, in-plane and perpendicular to the ring, of the spin-density map reconstructed onto the CNSSN^\bullet ring using an analytical model. By this method, the calculated magnetic structure factors, F_M^{calc} , are analytical functions of the spin populations and radial and orbital coefficients of the Slater wave functions. From F_N^{calc} , obtained from the low-temperature nuclear structure and F_M^{calc} the theoretical flipping ratios are calculated. By means of a least-square procedure, these theoretical flipping ratios are fitted to the experimental ones obtained in the polarised neutron diffraction experiment using a modification of the MOLLY program [11,12]. The Slater radial exponents are taken from Ref. [13]. In our refinements, the shape of the spin-density distribution has been refined in terms of a multipolar model.

As can be observed in Fig. 2(A) and (B), high-level and low-level contours plots, respectively, most of the spin density is carried by the CNSSN^\bullet ring. Positive populations are found on the nitrogen and sulphur atoms ($0.281\mu_B$ and $0.247\mu_B$, respectively) whereas in carbon atom a small and negative population is

Table 1
Atomic Mulliken populations (μ_B) for the $p\text{-O}_2\text{N}\cdot\text{C}_6\text{F}_4\cdot\text{CNSSN}^\bullet$ radical calculated from ab initio methods

Atom	PND	DMOL3
S1	0.281	0.320
N2	0.247	0.213
C5	-0.055	-0.063
C4		0.005
C3		-0.003
C2		0.002
C1		-0.003
F2		0.000
F1		0.000
N1		0.001
O1		0.000

The neutron experimental results are also shown.

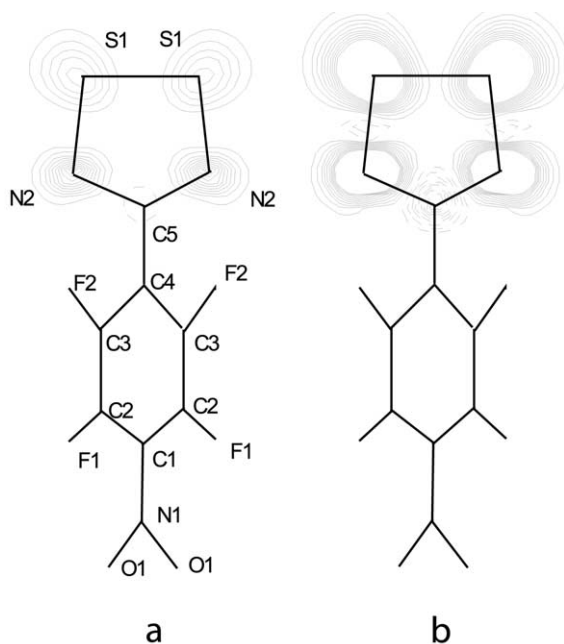


Fig. 2. Spin-density reconstruction of $\text{O}_2\text{N}\cdot\text{C}_6\text{F}_4\cdot\text{CNSSN}\cdot$ radical projected along the perpendicular to the CNSSN mean plane. The straight and dashed lines indicate, respectively, positive and negative contours levels. (A) High level, $0.05\mu_{\text{B}} \text{ \AA}^{-2}$, contours plots. (B) Low level, $0.01\mu_{\text{B}} \text{ \AA}^{-2}$, contours plots.

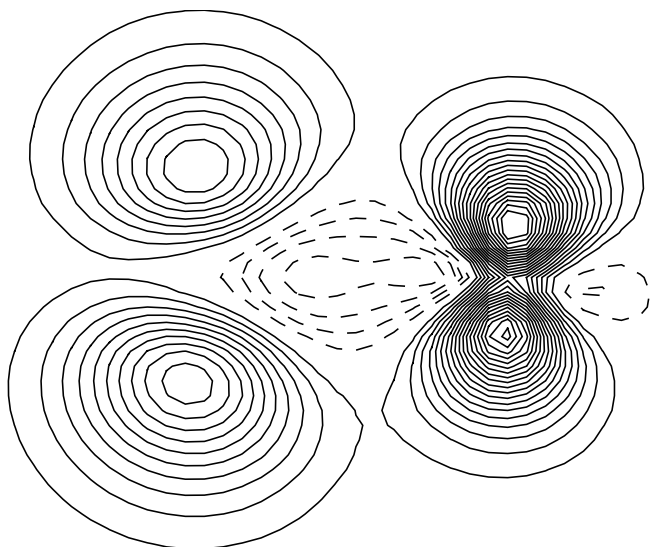


Fig. 3. Spin-density reconstruction projected along the S–N direction. Level, $0.02\mu_{\text{B}} \text{ \AA}^{-2}$, contours plots. The straight and dashed lines indicate, respectively, positive and negative contours levels.

observed ($-0.055\mu_{\text{B}}$). Some negative density is observed between the sulphur and nitrogen atoms that can be due to covalence and polarisation effects [14]. The spin density determined in the rest of the radical is below the limits of the experimental accuracy. The goodness-of-fit parameter χ^2 was 2.4 for the best-fit.

We found that most of the spin density is located in the atomic orbital perpendicular to the CNSSN• ring—

see Fig. 3 where the spin distribution is projected onto the plane perpendicular to the ring. We can then conclude that the unpaired electron is almost located in the π^* molecular orbital, in good agreement with theoretical calculations [15].

Our DFT calculations reproduce the same relevant facts, i.e. positive populations on sulphur and nitrogen atoms and negative for the carbon atom on the CNSSN• ring. Comparing the ab initio and experimental values, we observe that the population obtained for the sulphur and carbon atom is around 14% larger in the calculated case while for the nitrogen atom we find a population smaller in 14% in the calculated case compared with the experimental value. For the aromatic part of the molecule, the calculated spin-density populations follow an alternate sequence of signs being the values very small. In the rest of atoms (F, O, N1) the spin population is negligible.

From a close inspection to the nuclear structure and to the spin-density distribution, we can propose the exchange pathways contributing to the ferromagnetic phase transition at $T_c = 1.3 \text{ K}$. Four equivalent N–S exchange pathways connect each CNSSN• ring to four different molecules in a arrangement giving a 3D network of propagating interactions. In each of these exchange pathways, a nitrogen p_z orbital is pointing to a neighbour p_z sulphur orbital almost orthogonal, favouring a ferromagnetic interaction. These exchange pathways are schematically represented in Fig. 1 as dotted lines. Another mechanism giving ferromagnetic interaction might be the small overlap between the p_z orbital of the N, where a positive spin density is found, and that the in σ -orbital plane localised in the same interacting neighbour thiazyl ring. This orbital carries a small negative population (see Fig. 3), which arises from combinations of p_x and p_y orbitals.

Acknowledgements

We would like to thank the EPSRC, the CICYT (Grant MAT2000-1388-C03-03) for financial support, and the ESF programme “Molecular Magnets” for partial support to the collaborative activities. The Institut Laue Langevin is acknowledged for neutron beam time allocation on D9 and D3 instruments. Some of us (J.L., J.C. and F.P.) wish to dedicate this paper to Prof. Domingo González on his retirement.

References

- [1] P. Lahti (Ed.), *Magnetic Properties of Organic Materials*, Marcel Dekker, New York, 1999.

- [2] M. Tamura, Y. Nakazawa, D. Shiomi, K. Nozawa, Y. Hosokoshi, M. Ishikawa, M. Takahashi, M. Kinoshita, *Chem. Phys. Lett.* 186 (1991) 401.
- [3] Y. Nakazawa, M. Tamura, N. Shirakawa, D. Shiomi, M. Takahashi, M. Kinoshita, M. Ishikawa, *Phys. Rev. B* 46 (1992) 8906.
- [4] R. Chiarelli, M.A. Novak, A. Rassat, J.L. Tholence, *Nature* 363 (1993) 147.
- [5] P.M. Allemand, K.C. Khemani, A. Koch, F. Wudl, K. Holczer, S. Donovan, G. Gruner, J.D. Thompson, *Science* 253 (1991) 301.
- [6] F. Palacio, G. Antorrena, M. Castro, R. Burriel, J.M. Rawson, J.N.B. Smith, N. Bricklebank, J. Novoa, C. Ritter, *Phys. Rev. Lett.* 79 (1997) 2336.
- [7] J.M. Rawson, C.M. Pask, F. Palacio, P. Oliete, C. Paulsen, A. Yamaguchi, R.D. Farley, in press.
- [8] J.C. Matthewman, P. Thompson, P.J. Brown, *J. Appl. Cryst.* 15 (1982) 167.
- [9] A.D. Becke, *Phys. Rev. A* 38 (1988) 3098.
- [10] (a) DMOL3, A Registered Software Product of Molecular Simulations, Inc.;
(b) B. Delley, *J. Chem. Phys.* 92 (1990) 508;
(c) B. Delley, *J. Phys. Chem.* 100 (1996) 6107.
- [11] N.K. Hansen, P. Coppens, *Acta Crystallogr., Sect. A* 34 (1978) 909.
- [12] E. Ressouche, Ph.D. Thesis, University of Grenoble, Grenoble, 1991.
- [13] N.J. Henre, R.F. Steward, J.A. Pople, *J. Chem. Phys.* 51 (1969) 57.
- [14] P. Becker, P. Coppens, *Acta Crystallogr., Sect. A* 41 (1985) 171.
- [15] J. Campbell, D. Klapstein, P.F. Bernath, W.M. Davis, R.T. Oakley, J.D. Goddard, *Inorg. Chem.* 35 (1996) 4264.